K-5-01 (Invited)
Extended Abstracts of the 2019 International Conference on Solid State Devices and Materials, Nagoya, 2019, pp469-470

# Advances in inversion channel diamond MOSFETs

Norio Tokuda[1,2], Tsubasa Matsumoto[1], Takao Inokuma[1], Satoshi Yamasaki[1,2], Hiromitsu Kato[2], Toshiharu Makino[2], Christoph E. Nebel[1,3],

[1] Kanazawa Univ.
Kakuma-machi
Kanazawa 920-1192, Japan
Phone: +81-76-234-4875 E-mail: tokuda@ec.t.kanazawa-u.ac.jp
[2] National Institute of Advanced Industrial Science and Technology
1-1-1, Umezono
Tsukuba 305-8568, Japan
[3] Fraunhofer Institute for Applied Solid State Physics
Freiburg, 79108, Germany

**Abstract**

**In 2016, we reported the first inversion channel diamond MOSFETs with normally-off operation and high on/off ratios of over $10^{10}$ [1]. Here, we precisely controlled two interface structures: pn-junctions using selective growth of heavily B doped on n-type diamond layer for the formation of source/drain and MOS interface using an atomic layer deposition of $Al_2O_3$ film on OH-terminated diamond (111) surface. The field-effect mobility $\mu_{FE}$ of the p-channel diamond MOSFET was 8 $cm^2$/Vs at the highest, which is much lower than the hole mobility of 6,300 $cm^2$/V·s at RT [2]. In this study, we investigated the interface state density $D_{it}$ dependence of $\mu_{FE}$ in inversion channel diamond MOSFETs. The $\mu_{FE}$ and $D_{it}$ were strongly inversely correlated and the maximum $\mu_{FE}$ of 20 $cm^2$/V·s was obtained in the diamond MOSFET with the minimum $D_{it}$ of $1 \times 10^{13}$ $cm^{-2}$·$eV^{-1}$. The high $D_{it}$ in the diamond MOSFETs suggests that most holes are trapped at the interface state as a key factor for carrier scattering. Thus, it is important for obtaining higher $\mu_{FE}$ of diamond MOSFETs to reduce $D_{it}$ as well as that of Si and SiC ones.**

## 1. Introduction

Carbon is a member of group IV with the least atomic number above Si. Diamond, of which crystal structure is same with that of silicon, has been expected to be the semiconductor material of the next-generation high-power and high-frequency devices because of the superior physical and electronic properties such as extremely high thermal conductivity (20 W/cm·K), carrier mobility (7,300 and 6,300 $cm^2$/V·s for electron and hole, respectively [2]), and breakdown field (10 MV/cm). Actually, there have been many reports about semiconductor devices using diamond for applications like power devices [3-9]. Here, the inversion channel MOSFET is the most important device, because it shows normally-off characteristics. Si MOSFETs and insulated-gate bipolar transistors (IGBTs) based on the MOS structure are widely used because they allow to control the electric power accurately with high tolerance. Recently, we reported the first inversion channel diamond MOSFET with normally-off property and a high on/off ratio of over $10^{10}$ [1]. However, the field effect mobility and the drain current density were only 8 $cm^2$/Vs and 1.6 mA/mm, respectively. We attribute the low mobility and the correlated low drain current density to the high interface-state density of $6\times10^{12}$ $cm^{-2}eV^{-1}$ which is the key factor for carrier scattering. In this study, we investigated the interface-state density ($D_{it}$) dependence of the carrier mobility ($\mu_{FE}$) in inversion channel diamond MOSFETs.

## 2. Experimental

Figure 1 shows a schematic image of the cross-sectional structure of the inversion channel diamond MOSFET fabricated on a high-pressure high-temperature (HPHT) synthetic Ib (111) semi-insulating single-crystal diamond substrate.

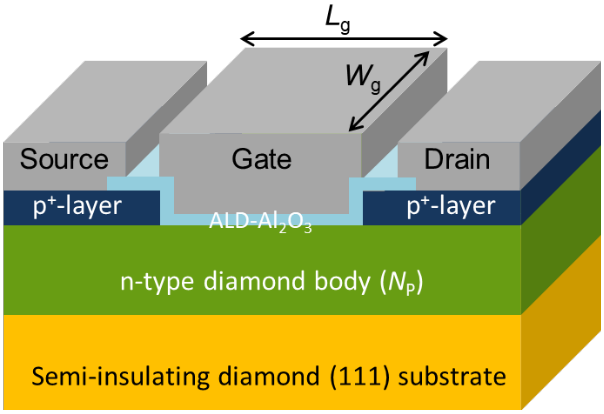


Fig. 1. Schematic image of the cross-sectional structure of an inversion channel diamond MOSFET on a high-pressure high-temperature (HPHT) synthetic Ib (111) semi-insulating single-crystal diamond substrate.

Here, $L_g$ and $W_g$ are the gate electrode length and width, respectively. The fabrication process was as follows. Firstly, Phosphorus (n)-doped diamond films as n-type bodies were grown onto each HPHT Ib (111) diamond substrate by microwave plasma-assisted (MP) chemical vapor deposition (CVD). The Phosphorus concentrations of the n-type bodies ($N_P$) were $2 \times 10^{15}$, $1 \times 10^{16}$, $3 \times 10^{16}$, and $6 \times 10^{16}$ $cm^{-3}$. Second, a $p^+$-type layer (Boron-doping) was selectively grown on each n-type body through a metal mask (Ti/Au) by MPCVD. The thickness and Boron concentration of the $p^+$-type layers were about 50 nm and about $10^{21}$ $cm^{-3}$, respectively. Third, after removing the metal mask by acid cleaning, the samples were treated by water vapor annealing in an electric furnace at 500 °C for 60 min under an atmosphere of $N_2$ gas bubbled through ultrapure water in a quartz tube to obtain stable OH surface terminations [10]. An $Al_2O_3$ films with 30~50 nm thick were then deposited onto each sample by atomic layer deposition (ALD) at 300 °C. When the $Al_2O_3$ layer was deposited, the termination of the diamond surface changed from OH to O because the chemical reaction between OH and trimethylaluminum is identical to that in the ALD mechanism. Gate, drain, and source electrodes (Ti/Pt/Au) were fabricated on each sample by photolithography and lift-off techniques. $L_g$ and $W_g$ were 15 and 100 µm, respectively.

## 3. Results and discussion

Figure 2 shows the drain current density ($I_d$) as a function of drain voltage ($V_{ds}$) for different gate potentials ($V_{gs}$) of the inversion channel diamond MOSFET with $N_P$ of 2 × $10^{15}$ $cm^{-3}$, $L_g$ of 15 µm, and $W_g$ of 100 µm measured in air at 300 K. We varied the gate voltage ($V_{gs}$) between 0 and -12 V with steps of -4 V. The drain source voltage was changed between 0 and -5 V with voltage steps of -0.1 V. The MOSFET exhibits normally-off properties and clear saturation characteristics. The drain current ($I_d$) is well modulated by the gate potential ($V_{gs}$). The maximum $I_d$ was -1.6 mA/mm. The threshold voltage $V_T$ is –0.9 V. The second MOSFET shows also normally-off properties as well as clear saturation characteristics (not shown here).

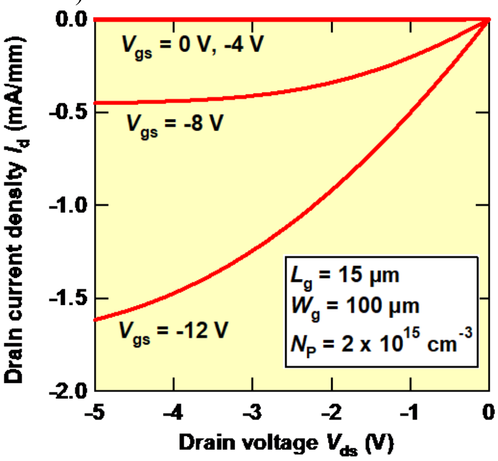


**Fig. 2.** $I_d$–$V_{ds}$ characteristics of the inversion channel diamond MOSFET with $N_P = 1 \times 10^{16}$ $cm^{-3}$, $L_g$ = 15 µm, and $W_g$ = 100 µm at RT. The applied $V_{gs}$ and $V_{ds}$ ranged from 0 to −12 V with a voltage step of −4 V and from 0 to −5 V with a voltage step of −0.1 V, respectively.

Figure 3 presents the summary of field effect mobilities ($\mu_{FE}$) as function of interface-state densities ($D_{it}$) measured at 300 K on the inversion channel diamond MOSFET and on 4H-SiC MOSFETs. Here, we use the maximum $\mu_{FE}$ of the diamond MOSFET because the applied $V_g$ is lower than applied on the 4H-SiC MOSFETs, and a clear saturation region is not observed. In addition, we plot $\mu_{FE}$ at $V_{gs}$–$V_T$ of -2 V for diamond, to focus on the low $V_{gs}$–$V_T$ region. The channel mobility $\mu_{FE}$ as plotted by triangles is inversely correlated with the interface state density $D_{it}$ values. The channel mobility plotted by squares decreases significantly faster with the channel defect density (see data $V_{gs}$- $V_T$ = −2 V for diamond). For example, when $D_{it}$ decreased to 1/3, $\mu_{FE}$ increases by a factor 100 in the low $V_{gs}$–$V_T$.

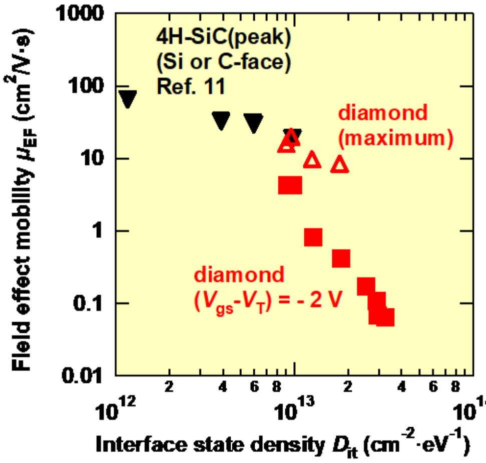


**Fig. 3.** Correlation between $\mu_{FE}$ and $D_{it}$ for the inversion channel diamond MOSFET and a 4H-SiC MOSFET [11]. The black triangles are the peak $\mu_{FE}$ of the 4H-SiC MOSFET, the filled red squares are the maximum $\mu_{FE}$ for the diamond MOSFET, and open red triangles are $\mu_{FE}$ at $V_{gs}$–$V_T$ of -2 V.

## 4. Conclusions

We successfully fabricated inversion channel diamond MOSFETs with normally-off characteristics and high on/off ratios using a high-quality insulated phosphorus doped n-type diamond body. The data reveal that the mobility of the inversion channel diamond MOSFETs are significantly affected by the (high) interface state densities and indicate the key problem for the realization of high-power and high-frequency diamond devices.

## Acknowledgements

This work was partially supported by Kanazawa University SAKIGAKE Project 2018 and JSPS KAKENHI Grant Numbers JP17H02786, 17H03248, 18KK0383, and 19K15042.

## References

[1] T. Matsumoto, N. Tokuda *et al.*, *Sci. Rep.* **6** (2016) 31585.
[2] I. Akimoto, N. Naka, N. Tokuda, *Diamond. Diamond Relat. Mater.* **63** (2016) 38.
[3] A. Traore *et al.*, *Appl. Phys. Lett.* **104** (20142) 052105.
[4] M. Suzuki *et al.*, *Phys. Status Solidi A* **210** (2013) 2035.
[5] N. Ozawa *et al.*, *Diamond Relat. Mater* **85** (2018) 49.
[6] D. Takeuchi *et al.*, *Jpn. J. Appl. Phys.* **51** (2012) 090113.
[7] H. Kawashima *et al.*, *Jpn. J. Appl. Phys.* **58** (2019) SBBD17.
[8] T. T. Pham *et al.*, *Appl. Phys. Lett.* **111** (2017) 173503.
[9] N. Oi *et al.*, *Sci. Rep.* **8** (2018) 10660.
[10] R. Yoshida, N. Tokuda *et al.*, *Appl. Surf. Sci.* **458** (2018) 222.
[11] H. Yoshioka *et al.*, *Appl. Phys. Lett.* **106** (2015) 109902.